

See discussions, stats, and author profiles for this publication at: <https://www.researchgate.net/publication/263944969>

Luminescence Properties of CdSe Quantum Dots: Role of Crystal Structure and Surface Composition

ARTICLE *in* JOURNAL OF PHYSICAL CHEMISTRY LETTERS · AUGUST 2013

Impact Factor: 7.46 · DOI: 10.1021/jz401198e

CITATIONS

21

READS

235

4 AUTHORS, INCLUDING:



[Subila kb](#)

Indian Institute Of Science Education and Res...

1 PUBLICATION 21 CITATIONS

[SEE PROFILE](#)



[G. Kishore Kumar](#)

Accenture

4 PUBLICATIONS 24 CITATIONS

[SEE PROFILE](#)



[Sonnada Math Shivaprasad](#)

Jawaharlal Nehru Centre for Advanced Scienti...

200 PUBLICATIONS 1,956 CITATIONS

[SEE PROFILE](#)

Luminescence Properties of CdSe Quantum Dots: Role of Crystal Structure and Surface Composition

K. B. Subila,[†] G. Kishore Kumar,[‡] S. M. Shivaprasad,^{*,‡} and K. George Thomas^{*,†,‡}

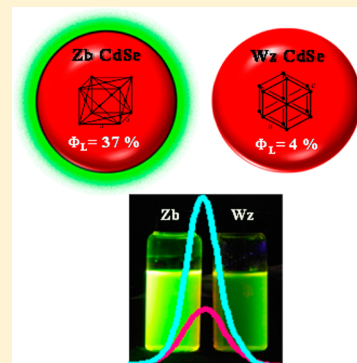
[†]School of Chemistry, Indian Institute of Science Education and Research Thiruvananthapuram (IISER-TVM), CET Campus, Thiruvananthapuram 695 016, India

[‡]Jawaharlal Nehru Centre for Advanced Scientific Research (JNCASR), Jakkur, Bangalore 560 064, India

Supporting Information

ABSTRACT: The crystal-structure-dependent luminescence properties of cadmium selenide quantum dots (QDs) in their cubic zincblende (*Zb*-CdSe) and hexagonal wurtzite (*Wz*-CdSe) phases have been investigated by maintaining their optical band gaps as well as the relative ratios of capping ligands the same. The *Zb*-CdSe QDs exhibited excellent photostability and high photoluminescence quantum yield ($\phi_L = 0.375$) compared with *Wz*-CdSe QDs ($\phi_L = 0.046$). Detailed X-ray photoelectron spectroscopic (XPS) investigation revealed an important finding that the surface of *Zb*-CdSe is rich with Cd²⁺ ions, which leads to the formation of CdO layer. This was further confirmed by analyzing the (i) Cd-to-Se stoichiometric ratio of zincblende QDs (2:1 on surface and 1:1 after sputtering) and (ii) core-level XPS spectra of oxygen. In contrast, the Cd-to-Se stoichiometric ratio was found to be same (1:1) for *Wz*-CdSe QDs throughout the crystal. Thus, the high luminescence of *Zb*-CdSe is attributed to the formation of a thin layer of CdO, leading to a type-I core–shell structure, which passivates the surface defects and confines the charge carriers. On the basis of the present investigation it is clear that the crystal structure plays a decisive role in modulating the surface properties of QDs, which determine the luminescence properties.

SECTION: Physical Processes in Nanomaterials and Nanostructures



Numerous synthetic approaches have been developed in the past decade on the design of highly monodisperse semiconductor nanocrystals, which have opened up a plethora of activities in various branches of science and technology.^{1–5} More importantly, understanding the quantum confinement effects in semiconductor nanocrystals allowed newer possibilities in tuning their physical properties by varying the size and shape.^{6,7} Another important factor that significantly influences the physical properties is their crystal structure.⁸ This knowledge is extremely important when various applications are concerned. For example, TiO₂ exists in three forms, namely, anatase, brookite, and rutile, among which the brookite phase exhibits markedly high photocatalytic activity.⁹ Another class of semiconductor system that has gained much attention is II–VI semiconductor systems (e.g., cadmium chalcogenides, such as CdS, CdSe, and CdTe) due to their potential applications as biological fluorescent labels^{10,11} and light-energy-harvesting systems.^{1–4} As far as these applications are concerned, luminescence properties play a crucial role; however, to the best of our knowledge there are no systematic attempts to understand crystal-structure-dependent luminescence properties of II–VI semiconductor nanocrystals.

The quantum dots (QDs) of CdS, CdSe, and CdTe mainly exist in two different crystalline forms: cubic zincblende and hexagonal wurtzite.¹² The atoms are tetrahedrally coordinated in both cases; however, they differ in the stacking sequence. Zincblende structure follows an ABCABC-type stacking along

the [111] direction, whereas an ABABAB stacking along the [0001] direction is observed in the wurtzite structure. Interestingly, thermodynamic stabilities of the two crystal structures of cadmium chalcogenides are different.¹³ In the case of CdS and CdSe, the thermodynamically stable phase is wurtzite, whereas zincblende is more stable in the case of CdTe.¹² The energy difference between the two forms is small, which often causes “polytypism” and poses difficulty in synthesizing their metastable phase in pure form.¹⁴ Successful attempts have been made for the synthesis of metastable phase of cadmium chalcogenides by involving (i) intelligent use of various capping agents¹⁵ (e.g., addition of trioctylphosphine, tetradecylphosphonic acid (TDPA)) and (ii) controlling the reaction temperature.^{16,17} Even though the methodologies for the synthesis of less common metastable phases are now well established,¹² the comparison of the crystal structure-dependent luminescence properties of cadmium chalcogenides are not well documented in a systematic fashion. In the present study, we have focused our investigations on CdSe QDs, and we have matched their optical band gaps for a meaningful comparison. The crystal-structure-dependent luminescence properties of CdSe QDs in its hexagonal wurtzite (*Wz*-CdSe) and cubic zincblende (*Zb*-CdSe) phases are presented.

Received: June 10, 2013

Accepted: August 1, 2013

Published: August 1, 2013

Both *Wz*-CdSe and *Zb*-CdSe QDs were synthesized by following a reported procedure¹⁸ with slight modifications, and details are provided in the Supporting Information. The size of both QDs is controlled during the synthesis in such a way that their optical band gaps are well matched. This is achieved by keeping the characteristic first excitonic peak centered at the same wavelength. Capping ligands on the surface can also influence the photophysical properties of QDs.¹⁹ Hence the synthetic procedures are modified in such a way that the relative ratios of various capping agents are the same in both crystal structures. It has been recently reported that the synthesis of high-quality CdSe QDs having zincblende structure can be achieved by adding TDPA to selenium precursor.¹⁸ In the present case, *Zb*-CdSe QDs were synthesized by heating the pot mixture containing cadmium precursor (consisting of CdO, oleic acid, and octadecene) to 240 °C under an argon atmosphere. A hot solution of selenium precursor, prepared by dissolving selenium (Se) in trioctylphosphine (TOP), octadecylamine (ODA), and TDPA, was injected to the above solution. The temperature of the reaction mixture was dropped to 210 °C, and this temperature was maintained throughout the course of crystal growth. It is relatively easy to synthesize CdSe QDs having wurtzite crystal structure by adopting high-temperature synthesis (>300 °C).^{20,21} In the present case, *Wz*-CdSe QDs were synthesized by adding TDPA along with the pot mixture containing cadmium precursor, maintaining the overall ratio of various capping agents the same as in the case of *Zb*-CdSe QDs. The reaction temperature was increased to 300 °C, and the hot selenium precursor was injected. Both *Wz*-CdSe and *Zb*-CdSe QDs were purified two times by precipitation from a mixture (1:1) of methanol and acetone, followed by centrifugation, and the residue was redispersed in chloroform for further studies. The weight ratios of ODA/OA/TDPA was kept as 3:2:2 during the synthesis in both cases, and the ligand coverage on the surface of QDs was further estimated using thermogravimetric analysis (Supporting Information). This was achieved by comparing the decomposition patterns of ligands bound on the surface of QDs with that of pure ligands. The weight ratios of ODA/OA/TDPA were found to be 2:5:8 for *Zb*-CdSe QDs and 1:5:10 for *Wz*-CdSe QDs. These results clearly indicate that the weight ratios of OA and TDPA on the surface of both QDs are more or less the same, whereas the relative amount of ODA is higher in *Zb*-CdSe QDs compared with that in *Wz*-CdSe QDs.

Both *Zb*-CdSe and *Wz*-CdSe QDs were further characterized by various spectroscopic and microscopic techniques and XRD analysis. The origin of various excitonic bands in the absorption spectrum of CdSe QDs is well established in the literature with the help of theoretical studies.²² These spectral features can provide insight into the crystal structure of CdSe QDs. It is reported that for a given particle size the energy difference between the first and the second excitonic bands (ΔE_{2-1}) is higher for the zincblende structure compared with that of wurtzite.^{23,24} The absorption spectrum (Figure 1A) of both wurtzite and zincblende QDs showed characteristic first excitonic peaks (543 nm for *Zb*-CdSe QDs and 540 nm for *Wz*-CdSe QDs). However, the higher excitonic features are distinctly different for both systems. It can be seen in Figure 1A (red trace) that the second and third excitonic peaks of *Zb*-CdSe QDs are well-defined. In contrast, the peak corresponding to the second excitonic band is not well-resolved in the case of *Wz*-CdSe and the third excitonic peak was found to be broad compared with that of zincblende analogue (blue trace). These

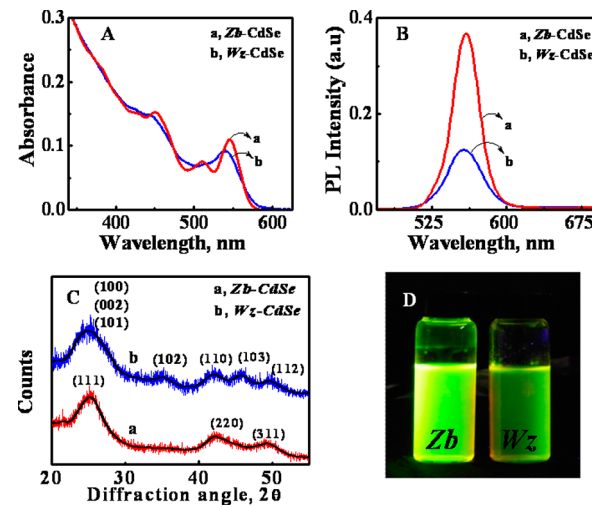


Figure 1. (A) Absorption and (B) photoluminescence spectra of optically matched solutions of *Zb*-CdSe QDs (trace a) and *Wz*-CdSe QDs (trace b) excited at 400 nm (OD = 0.18). (C) XRD pattern of *Zb*-CdSe (red trace, a) and *Wz*-CdSe (blue trace, b) and (D) photographs of *Zb*-CdSe and *Wz*-CdSe QDs under UV light.

results are consistent with previous reports²⁵ indicating the formation of *Wz*-CdSe and *Zb*-CdSe QDs.

The crystal structures of QDs were further confirmed by XRD analysis, and the results are presented as Figure 1C. The diffraction pattern of *Zb*-CdSe (red trace) showed three distinct peaks: the peak at a diffraction angle of $2\theta \approx 25^\circ$ is attributed to the (111) reflection, and the two broad peaks positioned at diffraction angles of $2\theta \approx 42^\circ$ and 50° correspond to (220) and (311) reflections, respectively (JCPDS file no. 19-0191). In the case of *Wz*-CdSe (blue trace), a shoulder was observed at a diffraction angle of $2\theta \approx 30^\circ$, which is attributed to the (002) plane (JCPDS file: 8-0459). The presence of the (102) reflection at $2\theta \approx 35^\circ$ and the (103) reflection at $2\theta \approx 46^\circ$ is also characteristic of the wurtzite lattice structure. The TEM image shown in Figure 2 indicates that both *Zb*-CdSe and *Wz*-CdSe QDs are highly crystalline and monodisperse. The average particle size is estimated as ~3.5 nm for *Zb*-CdSe and ~3.8 nm for *Wz*-CdSe QDs. Both QDs showed narrow band-edge emission with a full width at half-maximum (fwhm) close to ~30 nm, further indicating a narrow size distribution (Figure 1B).

The major focus of the present investigation is to understand the photoluminescence (PL) properties of CdSe QDs as a function of crystal structure. The PL spectra of optically matched solutions of *Zb*-CdSe and *Wz*-CdSe QDs, excited at 400 nm, are presented as Figure 1B. Interestingly, the PL of *Zb*-CdSe QDs is much higher than that of *Wz*-CdSe QDs, and this is also evident from the photographs presented as Figure 1D. Luminescence quantum yields (ϕ_L) of both *Zb*-CdSe and *Wz*-CdSe QDs in chloroform were estimated using fluorescein isothiocyanate (FITC) as standard ($\phi_f = 0.93$).²⁶ Three different batches of *Zb*-CdSe and *Wz*-CdSe QDs were synthesized independently, and the ϕ_L measurements were performed. These results are summarized as Supporting Information. The *Zb*-CdSe exhibited high luminescence quantum yield of 0.375 ± 0.008 as compared to *Wz*-CdSe QDs (0.046 ± 0.001). The differences in ϕ_L observed between the three different batches are very minimal, indicating that the

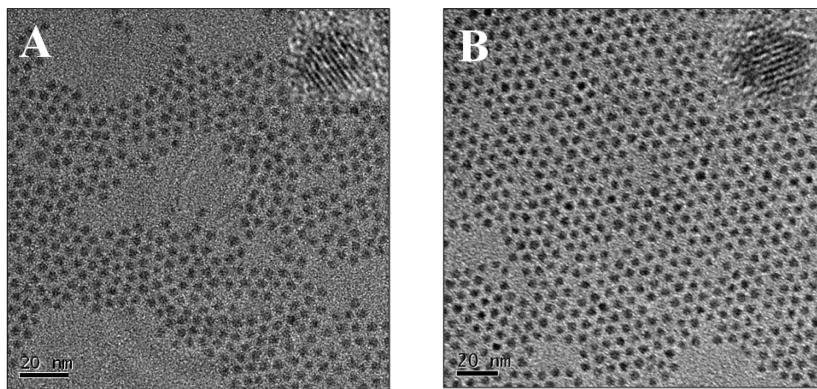


Figure 2. TEM images of (A) Zb-CdSe QDs and (B) Wz-CdSe QDs. Inset shows the high-resolution image of the corresponding system.

synthetic procedure followed in the present investigation is highly consistent and reproducible.

Photostability of QDs is another important criterion that needs to be considered while using them for various applications. We have further investigated the stability of both Zb-CdSe and Wz-CdSe QDs, and the results are presented as Figure 3. Optically matched solutions of QDs in chloroform

properties is extremely important for designing QDs as biological fluorescent labels^{10,11} and light-energy-harvesting systems.^{1–4} Nanocrystals possess large surface-to-volume ratio, and it is well documented that the surface defects have tremendous influence on their optical properties.²⁹ Extensive X-ray photoelectron spectroscopy (XPS) studies have been further carried out to unravel the surface properties of these QDs.

XPS can provide detailed information on (i) the nature of the elements on the surface of QDs, (ii) their percentage composition, and (iii) the chemical state of the constituent elements.³⁰ The binding energies of cadmium $3d_{5/2}$ and $3d_{3/2}$ electrons in bulk CdSe are reported at 405 and 412 eV, respectively, and 54 eV for selenium 3d electrons.³¹ The Cd and Se 3d core-level spectra of Zb-CdSe QDs are presented in Figure 4A,B and Wz-CdSe in Figure 4C,D. In the present case, the core-level spectra of $Cd_{5/2}$ and $Cd_{3/2}$ electrons of both Zb-CdSe and Wz-CdSe QDs are observed at binding energies of 405 eV and 411 eV, respectively. These spectra after Shirley background subtraction were deconvoluted into Gaussian components to provide information about the different chemical states of Cd and Se atoms present in the QDs. The cadmium atom present in the surface of CdSe QDs can be generally categorized as Cd bound to (i) selenium (Cd_S) and (ii) other elements (Cd_E). The peak correspond to the Cd atoms bound to Se atoms is represented by the blue trace in Figure 4A,C. Other peaks, arising from the surface Cd ions bound to various organic capping ligands, are represented by the green trace in Figure 4A,C. In both crystal structures, the contribution to Se signal arises from the 3d core electrons.

We have estimated the ratio of the Cd_S (cadmium bound to selenium) to Cd_E (cadmium bound to other elements) from the integrated Cd 3d signals using the appropriate sensitivity factor for each transition. The XPS composition analysis of both QDs is presented in the Supporting Information. In the case of Zb-CdSe QDs, the Cd_E/Cd_S ratio was found to be 1.50, while the ratio was 0.55 for Wz-CdSe QDs, indicating that the surface of Zb-CdSe QDs is approximately three times richer with Cd ions bound to other elements. Another interesting observation is the presence of additional peaks in the Cd $3d_{3/2}$ and $3d_{5/2}$ core-level spectra of Zb-CdSe QDs (green traces marked by asterisk, Figure 4A), which are blue-shifted by ~ 2 eV from the signal of Cd_S and ~ 1 eV from the Cd_E . These peaks can be attributed to the oxidized form of Cd atom, suggesting the presence of CdO surface layer.^{32,33} The formation of an oxide layer was further analyzed by following the XPS spectra of the 1s level of oxygen in both Zb-CdSe and

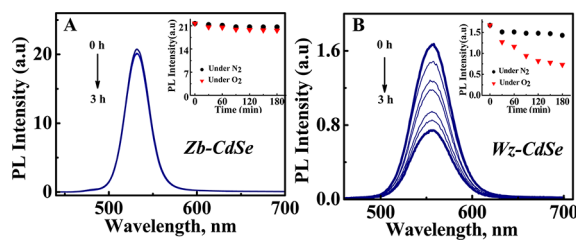


Figure 3. Photoluminescence spectra of optically matched solutions of (A) Zb-CdSe and (B) Wz-CdSe QDs in chloroform, under an oxygen atmosphere, measured as a function of time (excited at 400 nm). Variation of PL intensity of QDs, under nitrogen and oxygen, as a function of time is presented as inset.

were purged separately with nitrogen and oxygen, and their PL measurements were carried out as a function of time. The PL intensity of Zb-CdSe QDs remains more or less unchanged under nitrogen and oxygen (Figure 3A). Comparison of PL intensity under nitrogen and oxygen atmosphere is presented as inset. In contrast, the PL intensity of Wz-CdSe, kept under oxygen, decreased to 50% within 3 h (Figure 3B). The long-term photostability measurements of both the QDs were also performed. The PL intensity of Zb-CdSe QDs, kept under ambient condition, remained unchanged even after 2 months, indicating its high photostability, and the results are presented as Supporting Information. This confirms that the Zb-CdSe QDs are highly photostable in comparison with Wz-CdSe QDs.

Two significant observations drawn from the above studies are: (i) the Zb-CdSe QDs exhibit high luminescence quantum yield compared with Wz-CdSe QDs and (ii) Zb-CdSe QDs are photostable under ambient conditions compared with Wz-CdSe QDs. These results clearly indicate that the crystal structure of CdSe significantly influences its PL as well as its stability. There are a few reports in the literature comparing the optical properties of zincblende and wurtzite CdSe QDs.^{27,28} In the present case, we have investigated the role of crystal structure on the PL of CdSe QDs by matching their optical band gap and using the same capping ligands. In fact, the information on the crystal-structure-dependent photophysical

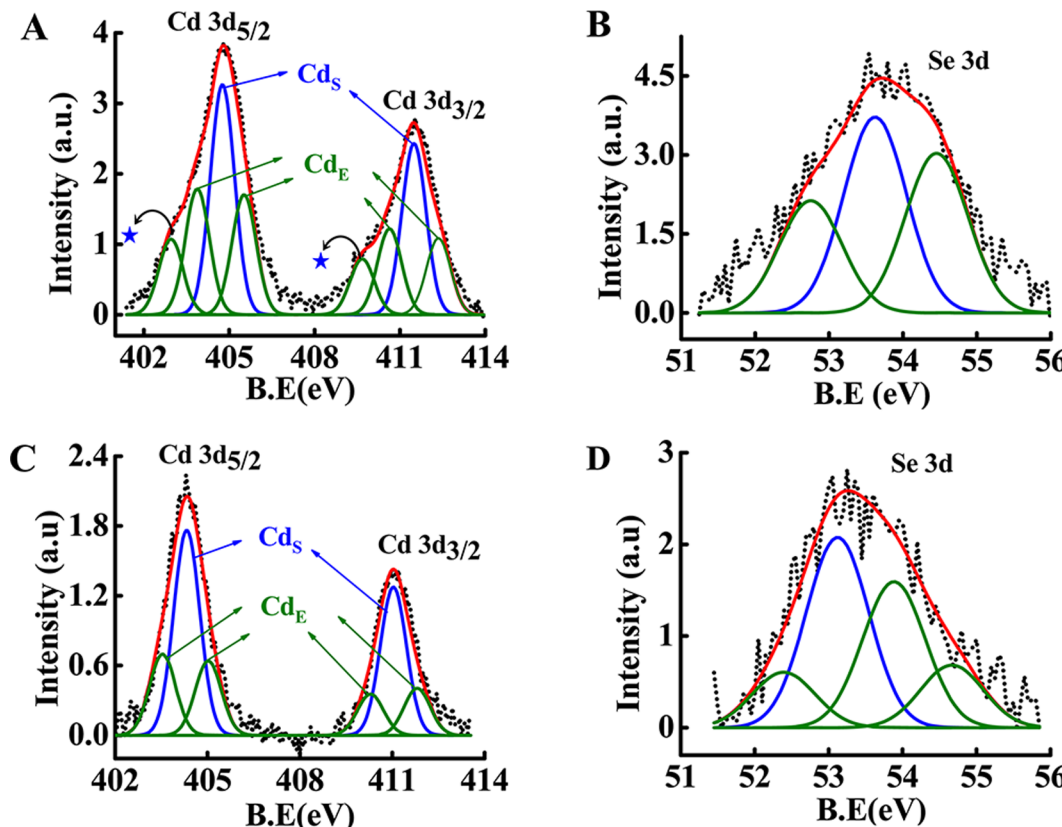


Figure 4. XPS counts from (A) Cd 3d electrons of Zb-CdSe, (B) Se 3d electrons of Zb-CdSe, (C) Cd 3d electrons of Wz-CdSe, and (D) Se 3d electron of Wz-CdSe. The experimental data as obtained are presented as black dotted traces and deconvoluted into Gaussian components. The peaks are characterized as (a) Cd bound to Se (blue traces) and (b) Cd bound to other elements (green traces; marked by asterisk represents Cd bound to oxygen). The red trace represents the Gaussian resultant fit.

Wz-CdSe QDs (Supporting Information). A significant broadening of the O 1s spectra was observed for Zb-CdSe as compared to that of Wz-CdSe QDs. The oxygen content in semiconductor QDs mainly arises from (i) adsorbed oxygen, (ii) oxygen atoms present in various capping ligands bound on the surface, and (iii) oxides of cadmium or selenium (CdO or SeO₂). The O 1s spectra of both Zb-CdSe and Wz-CdSe QDs were deconvoluted into Gaussian components, which can provide information about the different chemical states of oxygen. It is reported in the literature that the peak at 532.5 eV in the O 1s spectra originates from the oxygen atom bound to Cd in the form of CdO.³⁴ Thus the blue-shifted peaks (green traces marked by asterisk, Figure 4A) in the Cd 3d level and the peak at 532.5 eV in the O 1s level confirm the presence of a CdO layer on the surface of Zb-CdSe QDs. In contrast, these peaks were not observed in the core-level spectra of the Cd 3d (Figure 4C) and O 1s (Supporting Information) of the wurtzite QDs, ruling out the possibility of the formation of CdO layer.

The Cd-to-Se stoichiometric ratios in the surface layer and at the core of both Zb-CdSe and Wz-CdSe QDs were further investigated by XPS analysis. The stoichiometric elemental ratio of the core was determined by sputtering experiments, that is, exposing the QDs to 1 keV Ar⁺ ions for 3 min, which removes the surface layer, allowing the composition analysis of the core. The Cd-to-Se ratio before sputtering was found to be ~2:1 for Zb-CdSe QDs and 1:1 for Wz-CdSe QDs (details are presented in the Supporting Information). Interestingly, the ratio of Cd to Se for Zb-CdSe in the core, after sputtering for 3 min, was found to be 1:1, whereas the ratio remains the same (1:1) for

Wz-CdSe QDs. These results are presented as Table 1. Thus, the stoichiometric elemental ratios based on XPS analysis

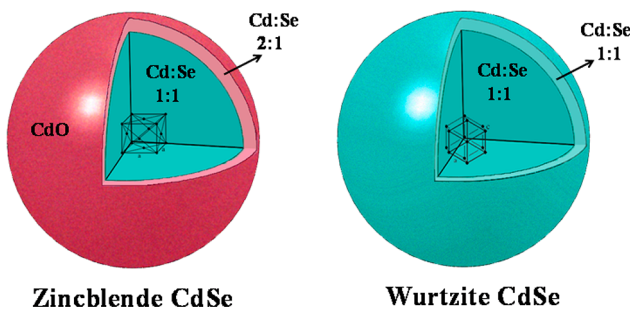
Table 1. Composition Analysis of CdSe Quantum Dots from XPS

CdSe	Cd/Se ratio	
	surface layer ^{a,b}	core ^{b,c}
Zb-CdSe	2:1	1:1
Wz-CdSe	1:1	1:1

^aBefore sputtering. ^bRatios are calculated based on the XPS composition analysis of Cd and Se (Supporting Information) ^cAfter sputtering for 3 min using 1 keV Ar⁺ ions,

confirm that the surface layer of Zb-CdSe QDs is rich in cadmium ions, resulting in the formation of a thin layer of CdO. In contrast, the Cd-to-Se ratio remains the same throughout the crystal lattice for Wz-CdSe QDs. Elemental distributions of Cd/Se for Zb-CdSe and Wz-CdSe QDs, based on XPS analysis, are presented as Scheme 1. It is reported that the overcoating of QDs with inorganic materials having larger band gap results in the formation of core/shell nanostructures (e.g., CdSe/ZnS, CdSe/CdS), generally termed as type-I systems.³⁵ Type-I core/shell systems are known to show high quantum efficiency due to the (i) robust passivation of the surface defects and (ii) strong confinement of charge carriers.^{36,37} In the present case, CdO layer formed on the surface of Zb-CdSe is a wide-band-gap material, having an energy offset of 2.32 eV.³⁸ The formation of CdO layer

Scheme 1. Schematic Representation of the Elemental Distribution in Zincblende and Wurtzite CdSe QDs based on the XPS Analysis



passivates the surface defects³⁹ and confines the charge carriers in the low-band-gap CdSe QDs (1.74 eV),⁴⁰ which results in high PL quantum yield in Zb-CdSe QDs.

It is clear from the present investigation that the Cd-to-Se ratio for Wz-CdSe QDs remains the same throughout the crystal and CdO layer is absent on the surface. It is reported in the literature that the PL intensity of semiconductor QDs dramatically enhances on treatment with reducing agents, for example, passivating the surface dangling bonds through coordination with hydrazine⁴¹ or treatment with NaBH₄, which results in the formation of an oxide layer.³³ We have further investigated the variation in PL intensity of both Zb-CdSe and Wz-CdSe QDs on treating with NaBH₄. An oxygen-saturated solution of QDs in chloroform was stirred for 1 h in the presence of NaBH₄ (1 wt %). In the case of Wz-CdSe QDs, the absorption spectrum underwent a blue shift of 8 nm followed, by large enhancement in the PL intensity (Supporting Information), which can be attributed to the modification of surface with CdO layer. Ligands having carboxylic acid functionality present on the QD surface get reduced to corresponding alcohols and lose their coordinating ability. Hence, oxygen can easily diffuse to the surface through the less dense surfactant layer, resulting in the formation of a thin oxide layer. These results are in accordance with that reported in the literature.³³ In contrast, Zb-CdSe QDs showed only negligible variation in PL intensity upon treatment with NaBH₄ (Supporting Information) because the surface is already passivated by a layer of CdO.

It is well established that the chemical composition on the surface of QDs has a dramatic effect on their PL properties.⁴² In a recent report, Heyes and coworkers⁴³ synthesized a series of CdTe QDs by varying the Cd-to-Te molar ratios and investigated the role of surface atoms and ligand functional groups on the radiative and nonradiative relaxation rates. The ratio of cadmium and tellurium ions on the surface was estimated from XPS. The identity of ligand molecules bound to each sample and their amount were determined by following the FTIR. It was found that the amount of TDPA on CdTe is high when the ratio of Cd to Te is 5:1, which substantially decreased when the ratio was 1:1. The authors conclude that the effective binding of ligands on to the Cd-rich surface of CdTe decreases the surface trap states, leading to high quantum efficiency. These studies are complementary to our findings that the Cd²⁺-rich surface of Zb-CdSe QDs forms a thin layer of CdO, which contributes to the high luminescence efficiency.

In summary, we have investigated the ratio of Cd to Se in the surface layer and core of both zincblende and wurtzite CdSe QDs using detailed XPS analysis. On the basis of these studies,

it is established that the surface of Zb-CdSe QDs is rich with Cd²⁺ ions, leading to the formation of a CdO layer as shell, which provides a better passivation and confines the charge carriers. The core–shell type structure formed in the case of Zb-CdSe QDs possesses excellent photostability and showed seven times higher PL efficiency than the Wz-CdSe QDs. Results presented here clearly indicate that Zb-CdSe QDs are ideal for various applications that demand high emission yield. The CdSe QDs being one of the widely used semiconductor systems, the fundamental understanding of the origin of crystal-structure-dependent luminescence is extremely useful for researchers working in broad areas of science and technology.

■ ASSOCIATED CONTENT

§ Supporting Information

Details of the synthetic procedures and XPS and TGA analysis. This material is available free of charge via the Internet at <http://pubs.acs.org>.

■ AUTHOR INFORMATION

Corresponding Author

*E-mail: kgt@iisertvm.ac.in (K.G.T.); smsprasad@jncasr.ac.in (S.M.S.).

Notes

The authors declare no competing financial interest.

■ ACKNOWLEDGMENTS

We thank Prof. C. N. R. Rao for all of the support and encouragement. Thanks are also due to Dr. Pratheesh V. Nair of IISER-TVM and Dr. Priya Mahadevan of S. N. Bose National Centre for Basic Science, Kolkata for their valuable suggestions. We thank IISER, Thiruvananthapuram and Department of Science and Technology, Government of India (DST-European Commission Project. INT/IRMC/EC-SOLAR/LARGECELLS:1/261936/2010) for financial support and NIIST (CSIR) Thiruvananthapuram for XRD and TEM analysis. K.B.S. thanks UGC for the fellowship.

■ REFERENCES

- (1) Kamat, P. V. Quantum Dot Solar Cells. The Next Big Thing in Photovoltaics. *J. Phys. Chem. Lett.* **2013**, *4*, 908–918.
- (2) Hetsch, F.; Xu, X.; Wang, H.; Kershaw, S. V.; Rogach, A. L. Semiconductor Nanocrystal Quantum Dots as Solar Cell Components and Photosensitizers: Material, Charge Transfer, and Separation Aspects of Some Device Topologies. *J. Phys. Chem. Lett.* **2011**, *2*, 1879–1887.
- (3) Tongying, P.; Plashnitsa, V. V.; Petchsang, N.; Vietmeyer, F.; Ferraudi, G. J.; Krylova, G.; Kuno, M. Photocatalytic Hydrogen Generation Efficiencies in One-Dimensional CdSe Heterostructures. *J. Phys. Chem. Lett.* **2012**, *3*, 3234–3240.
- (4) MacDonald, B. I.; Martucci, A.; Rubanov, S.; Watkins, S. E.; Mulvaney, P.; Jasieniak, J. J. Layer-by-Layer Assembly of Sintered CdSe_xTe_{1-x} Nanocrystal Solar Cells. *ACS Nano* **2012**, *6*, 5995–6004.
- (5) Liu, X. M.; Tomita, Y.; Oshima, J.; Chikama, K.; Matsubara, K.; Nakashima, T.; Kawai, T. Holographic Assembly of Semiconductor CdSe Quantum Dots in Polymer for Volume Bragg Grating Structures with Diffraction Efficiency Near 100%. *Appl. Phys. Lett.* **2009**, *95*, 261109.
- (6) Alivisatos, A. P. Perspectives on the Physical Chemistry of Semiconductor Nanocrystals. *J. Phys. Chem.* **1996**, *100*, 13226–13239.
- (7) Nirmal, M.; Brus, L. Luminescence Photophysics in Semiconductor Nanocrystals. *Acc. Chem. Res.* **1998**, *32*, 407–414.
- (8) Nag, A.; Hazarika, A.; Shanavas, K. V.; Sharma, S. M.; Dasgupta, I.; Sarma, D. D. Crystal Structure Engineering by Fine-Tuning the

- Surface Energy: The Case of CdE ($E = S/Se$) Nanocrystals. *J. Phys. Chem. Lett.* **2011**, *2*, 706–712.
- (9) Kandiel, T. A.; Robben, L.; Alkaim, A.; Bahnenmann, D. Brookite versus Anatase TiO_2 Photocatalysts: Phase Transformations and Photocatalytic Activities. *Photochem. Photobiol. Sci.* **2013**, *12*, 602–609.
- (10) Bruchez, M.; Moronne, M.; Gin, P.; Weiss, S.; Alivisatos, A. P. Semiconductor Nanocrystals as Fluorescent Biological Labels. *Science* **1998**, *281*, 2013–2016.
- (11) Chan, W. C. W.; Nie, S. Quantum Dot Bioconjugates for Ultrasensitive Nonisotopic Detection. *Science* **1998**, *281*, 2016–2018.
- (12) Wei, S.-H.; Zhang, S. B. Structure Stability and Carrier Localization in CdX ($X=S, Se, Te$) Semiconductors. *Phys. Rev. B* **2000**, *62*, 6944–6947.
- (13) Manna, L.; Milliron, D. J.; Meisel, A.; Scher, E. C.; Alivisatos, A. P. Controlled Growth of Tetrapod-Branched Inorganic Nanocrystals. *Nat. Mater.* **2003**, *2*, 382–385.
- (14) Mahler, B.; Lequeux, N.; Dubertret, B. Ligand-Controlled Polytypism of Thick-Shell CdSe/CdS Nanocrystals. *J. Am. Chem. Soc.* **2009**, *132*, 953–959.
- (15) Washington, A. L.; Foley, M. E.; Cheong, S.; Quiffa, L.; Breshike, C. J.; Watt, J.; Tilley, R. D.; Strouse, G. F. Ostwald's Rule of Stages and Its Role in CdSe Quantum Dot Crystallization. *J. Am. Chem. Soc.* **2012**, *134*, 17046–17052.
- (16) Cao, Y. C.; Wang, J. One-Pot Synthesis of High-Quality Zinc-Blende CdS Nanocrystals. *J. Am. Chem. Soc.* **2004**, *126*, 14336–14337.
- (17) Nan, W.; Niu, Y.; Qin, H.; Cui, F.; Yang, Y.; Lai, R.; Lin, W.; Peng, X. Crystal Structure Control of Zinc-Blende CdSe/CdS Core/Shell Nanocrystals: Synthesis and Structure-Dependent Optical Properties. *J. Am. Chem. Soc.* **2012**, *134*, 19685–19693.
- (18) Mohamed, M. B.; Tonti, D.; Al-Salman, A.; Chemseddine, A.; Chergui, M. Synthesis of High Quality Zinc Blende CdSe Nanocrystals. *J. Phys. Chem. B* **2005**, *109*, 10533–10537.
- (19) Frederick, M. T.; Amin, V. A.; Weiss, E. A. Optical Properties of Strongly Coupled Quantum Dot–Ligand Systems. *J. Phys. Chem. Lett.* **2013**, *4*, 634–640.
- (20) Talapin, D. V.; Rogach, A. L.; Kornowski, A.; Haase, M.; Weller, H. Highly Luminescent Monodisperse CdSe and CdSe/ZnS Nanocrystals Synthesized in a Hexadecylamine–Trioctylphosphine Oxide–Trioctylphosphine Mixture. *Nano Lett.* **2001**, *1*, 207–211.
- (21) Talapin, D. V.; Rogach, A. L.; Mekis, I.; Haubold, S.; Kornowski, A.; Haase, M.; Weller, H. Synthesis and Surface Modification of Amino-Stabilized CdSe, CdTe and InP Nanocrystals. *Colloids Surf., A* **2002**, *202*, 145–154.
- (22) Scholes, G. D. Controlling the Optical Properties of Inorganic Nanoparticles. *Adv. Funct. Mater.* **2008**, *18*, 1157–1172.
- (23) Norris, D. J.; Bawendi, M. G. Measurement and Assignment of the Size-Dependent Optical Spectrum in CdSe Quantum Dots. *Phys. Rev. B* **1996**, *53*, 16338–16346.
- (24) Jasieniak, J.; Bullen, C.; van Embden, J.; Mulvaney, P. Phosphine-Free Synthesis of CdSe Nanocrystals. *J. Phys. Chem. B* **2005**, *109*, 20665–20668.
- (25) Talapin, D. V.; Nelson, J. H.; Shevchenko, E. V.; Aloni, S.; Sadler, B.; Alivisatos, A. P. Seeded Growth of Highly Luminescent CdSe/CdS Nanoheterostructures with Rod and Tetrapod Morphologies. *Nano Lett.* **2007**, *7*, 2951–2959.
- (26) Velapoldi, R. A.; Tonnesen, H. H. Corrected Emission Spectra and Quantum Yields for a Series of Fluorescent Compounds in the Visible Spectral Region. *J. Fluoresc.* **2004**, *14*, 465–472.
- (27) Xia, X.; Liu, Z.; Du, G.; Li, Y.; Ma, M. Wurtzite and Zinc-Blende CdSe Based Core/Shell Semiconductor Nanocrystals: Structure, Morphology and Photoluminescence. *J. Lumin.* **2010**, *130*, 1285–1291.
- (28) Karel Čapek, R.; Moreels, I.; Lambert, K.; DeMuynck, D.; Zhao, Q.; Van Tomme, A.; Vanhaecke, F.; Hens, Z. Optical Properties of Zincblende Cadmium Selenide Quantum Dots. *J. Phys. Chem. C* **2010**, *114*, 6371–6376.
- (29) Nanda, J.; Kuruvilla, B. A.; Sarma, D. D. Photoelectron Spectroscopic Study of CdS Nanocrystallites. *Phys. Rev. B* **1999**, *59*, 7473–7479.
- (30) Wagner, C. D.; Riggs, W. M.; Davis, L. E.; Moulder, J. F.; Muilenberg, G. E. *Handbook of X-ray Photoelectron Spectroscopy*; Physical Electronics Division, Perkin-Elmer: Eden Prairie, MN; 1979.
- (31) Katari, J. E. B.; Colvin, V. L.; Alivisatos, A. P. X-ray Photoelectron Spectroscopy of CdSe Nanocrystals with Applications to Studies of the Nanocrystal Surface. *J. Phys. Chem.* **1994**, *98*, 4109–4117.
- (32) Setty, M. S.; Sinha, A. P. B. Characterization of Highly Conducting PbO Doped Cd_2SnO_4 Thick Films. *Thin Solid Films* **1986**, *144*, 7–19.
- (33) Jang, E.; Jun, S.; Chung, Y.; Pu, L. Surface Treatment to Enhance the Quantum Efficiency of Semiconductor Nanocrystals. *J. Phys. Chem. B* **2004**, *108*, 4597–4600.
- (34) Saha, B.; Das, S.; Chattopadhyay, K. K. Electrical and Optical Properties of Al Doped Cadmium Oxide Thin Films Deposited by Radio Frequency Magnetron Sputtering. *Sol. Energy Mater. Sol.* **2007**, *91*, 1692–1697.
- (35) Hines, M. A.; Guyot-Sionnest, P. Synthesis and Characterization of Strongly Luminescing ZnS-Capped CdSe Nanocrystals. *J. Phys. Chem.* **1996**, *100*, 468–471.
- (36) Dabbousi, B. O.; Rodriguez-Viejo, J.; Mikulec, F. V.; Heine, J. R.; Mattoussi, H.; Ober, R.; Jensen, K. F.; Bawendi, M. G. CdSe/ZnS Core–Shell Quantum Dots: Synthesis and Characterization of a Size Series of Highly Luminescent Nanocrystallites. *J. Phys. Chem. B* **1997**, *101*, 9463–9475.
- (37) Peng, X.; Schlamp, M. C.; Kadavanich, A. V.; Alivisatos, A. P. Epitaxial Growth of Highly Luminescent CdSe/CdS Core/Shell Nanocrystals with Photostability and Electronic Accessibility. *J. Am. Chem. Soc.* **1997**, *119*, 7019–7029.
- (38) Gurumurugan, K.; Mangalaraj, D.; Narayandass, S. K.; Balasubramanian, C. Structural, Optical, and Electrical Properties of Cadmium Oxide Films Deposited by Spray Pyrolysis. *Phys. Status Solidi A* **1994**, *143*, 85–91.
- (39) Lee, W.; Hoechang, K.; Jung, D. R.; Kim, J.; Nahm, C.; Lee, J.; Kang, S.; Park, B.; Lee, B. An Effective Oxidation Approach for Luminescence Enhancement in CdS Quantum Dots by H_2O_2 . *Nanoscale Res. Lett.* **2012**, *7*, 672.
- (40) Reiss, P.; Protière, M.; Li, L. Core/Shell Semiconductor Nanocrystals. *Small* **2009**, *5*, 154–168.
- (41) Nair, P. V.; Thomas, K. G. Hydrazine-Induced Room-Temperature Transformation of CdTe Nanoparticles to Nanowires. *J. Phys. Chem. Lett.* **2010**, *1*, 2094–2098.
- (42) Wei, H. H.; Evans, C. M.; Swartz, B. D.; Neukirch, A. J.; Young, J.; Prezhdo, O. V.; Krauss, T. D. Colloidal Semiconductor Quantum Dots with Tunable Surface Composition. *Nano Lett.* **2012**, *12*, 4465–4471.
- (43) Omogo, B.; Aldana, J. F.; Heyes, C. D. Radiative and Nonradiative Lifetime Engineering of Quantum Dots in Multiple Solvents by Surface Atom Stoichiometry and Ligands. *J. Phys. Chem. C* **2013**, *117*, 2317–2327.

■ NOTE ADDED AFTER ASAP PUBLICATION

This Letter was published on August 1, 2013, with an incorrect title in ref 41 and incorrect journal in ref 43. The corrected version was reposted on August 15, 2013.